Matched-field Source Localization via Statistical Covariance Matching

Yue Zhou and Wen Xu*
Department of Information Science and Electronic Engineering
Zhejiang University
Hangzhou, 310027, China
*Email: wxu@zju.edu.cn

***Abstract*—Matched-field methods concern estimation of source locations and/or ocean environmental parameters by exploiting full wave modeling of acoustic waveguide propagation. Typical estimation performance demonstrates that sidelobe ambiguities dominate the estimation at low signal-to-noise ratio (SNR), leading to a threshold performance behavior. An adaptive estimator, such as minimum variance distortionless response (MVDR), has the estimate-subtract structure, which can lead to the sidelobe suppression. However, in practical circumstances, the lack of snapshots would cause dramatic performance deterioration of MVDR. In this paper, we bring in a new matched-covariance estimator (MCE) into matched-field processing (MFP) to attack such weakness. Performance analysis of MCE is implemented for source localization in a typical shallow water environment chosen from the 2001 Asian Seas International Acoustic Experiment (ASIAEX). Simulation results demonstrate that 1) MCE owns the resolution benefit of an adaptive method while being robust against snapshot deficiency; 2) in terms of MSE, it performs almost equally well with the maximum likelihood estimator (MLE) and can outperform the MVDR; 3) for the threshold SNR concern, MCE has a threshold SNR close to that of the MLE and much lower than that of the MVDR. Overall, MCE achieves a trade-off between spatial resolution and snapshot-number robustness.**

***Index Terms*—Matched field processing, statistical signal model, matched-covariance estimator, threshold phenomenon, sidelobe cancellation.**

I. Introduction

Matched-field processing (MFP) is a parameter estimation technique which concerns estimation of source location and/or ocean environmental parameters by exploiting full wave modeling of acoustic waveguide propagation [1]. For this parameter estimation problem, some performance bounds on the mean square error (MSE) have been developed along with the estimation method [2], which specifie the fundamental performance under the given physical model.The well known maximum-likelihood estimator (MLE) is a form of the conventional matched-field processor under spatially white noise field [3], which can approach the Cramer-Rao lower bound (CRB) for sufficiently high (signal-to-noise ratio) SNR or long observation time [4]. Signal ambiguity function is a measure of the invertibility of the signal field and its output is the ambiguity surface which is often characterized by a multi-model structure [5]. For MLE, in addition to the wide mainlobe around the true parameter, there are many high level sidelobes in the ambiguity surface. To focus the mainlobe and to reduce the sidelobes leakage, some adaptive estimators, based on both the steering vector and the data, have been proposed. The standard adaptive MFP processor, known as minimum variance distortionless response (MVDR), has the estimate-subtract structure, which can lead to sidelobe suppression. However in practical circumstances, using sample covariance calculated with a finite number of snapshots, instead of the ensemble one, may result in performance deterioration even when the sample covariance has full rank.

In Ref. [5], a new estimator has been derived from the Weiss-Weinstein bound (WWB). Applications of this new estimator (now termed matched-covariance estimator, MCE) to sensor array bearing estimation have demonstrated some nice features, such as owning a high resolution of an adaptive method while being robust against snapshot deficiency.

In this paper, we bring in the new estimator matched-covariance estimator into the source localization problem and analyze its performance in MFP framework. Some major assumptions on signal/noise processes involved in the matched-field problem are firstly discussed in section II and following that a description of the embedded structure in the Weiss-Weinstein bound is given. Via a comparison between MVDR and WWB, MCE is presented in section IV. Then the performance of MCE against MVDR and MLE in source localization is analyzed via simulations in a realistic shallow water environment, which is constructed based on inversion results from the Asian Seas International Acoustic Experiment (ASIAEX) [6]. Finally, Section VI summarizes the paper.

II. Matched-Field Problem

Consider a stratified waveguide model for the seismo/acoustic environment, which consists of a water column, multilayer sediment and semi-infinite basement, and can be either range-dependent or independent (see Fig. 1 for an example). A point source radiates narrowband or broadband signals and the signal field is sampled by a vertical line array. We denote the unknown parameter set by a real vector $\boldsymbol{\theta}$ and its dimension by N_P. Typically, this parameter set may include source position (range, depth, and bearing) and/or environmental parameters (e.g., bathymetry, sound-speed, attenuation, and density). Similar to performance analysis of matched-field methods in [7] we use a data model of random signal embedded in random noise. The major

978-0-933957-40-4 ©2013 MTS

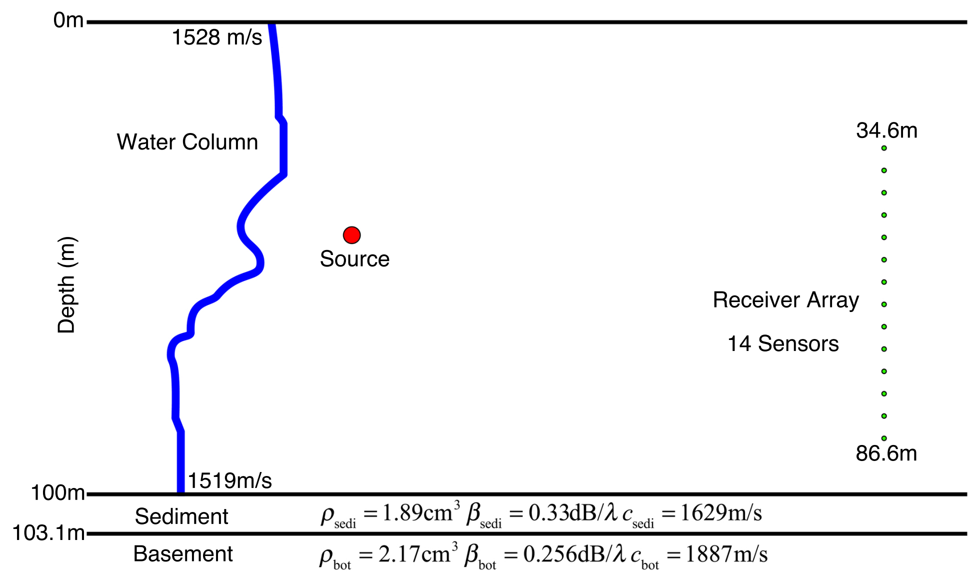

Fig. 1. Shallow water environmental with depth dependent sound-speed profile [6]. Source-receiver configuration is also shown.

assumptions on signal/noise/environment processes are listed here:

1) The signal source is a stationary random process. We use a complex Gaussian random variable $\widetilde{b}_l$ with variance σ_b^2 to scale and present the uncertainty.
2) Both the signal and noise processes follow a zero-mean complex circular Gaussian distribution.
3) For each frequency bin, we have a number of snapshots. The number of snapshots is determined by the total observation time and the correlation time of the source process.
4) Moving source would limit the number of snapshots available for calculating the sample covariance matrix. Though the MCE is robust with the snapshot deficiency, we still dismiss the source motion effect for the purpose of performance comparison.
5) We consider only the sensor noise which is an independent and spatial white random process. The covariance of the noise process is represented as σ_{wn}^2
6) Environmental variation is stationary. For a short observation time, this assumption usually stays true.

Suppose we have L independent measurements for each of M frequencies $f_m, m = 1, 2, ..., M$. The complex envelope of the received signal at each frequency bin can thus be expressed as [8]

$$\mathbf{R}_l\left(f_m, \boldsymbol{\theta}\right) = \widetilde{b}_l\left(f_m\right) \mathbf{G}\left(f_m, \boldsymbol{\theta}\right) + \mathbf{n}_l\left(f_m\right), \qquad l = 1, 2, ...L \quad m = 1, ...M \tag{1}$$

where

$\mathbf{R}_l\left(f_m, \boldsymbol{\theta}\right)$ is an $N \times 1$ vector representing the lth snapshot and N is the number of hydrophones;
$\mathbf{G}\left(f_m, \boldsymbol{\theta}\right)$ is a vector of Green function for the propagation from the source to the hydrophones;
$\mathbf{n}_l\left(f_m\right)$ is the lth snapshot of the stationary noise vector.

Note that

$$\mathbf{R} = \left[\mathbf{R}_1^T(f_1) \ldots \mathbf{R}_1^T(f_M) \ldots \mathbf{R}_l^T(f_1) \ldots \mathbf{R}_l^T(f_M)\right]^T, \tag{2}$$

where $(\ )^T$ represents the matrix transpose operation. Since $\mathbf{R}_l$ are uncorrelated across frequencies and snapshots, the covariance matrix of $\mathbf{R}_l\left(f_m, \boldsymbol{\theta}\right)$ is given by

$$\mathbf{K}_{\mathbf{R}} = \sigma_b^2 \mathbf{G}\left(f_m, \boldsymbol{\theta}\right) \mathbf{G}(f_m, \boldsymbol{\theta})^H + \sigma_{wn}^2 \mathbf{I}. \tag{3}$$

III. The Weiss-Weinstein Bound

As a global bound, the WWB can predict the MLE performance tightly at all SNR regions [5]. The WWB is defined by [9]

$$\boldsymbol{\Sigma} \geq \max_{\{s_j, h_j\}} \mathbf{H}\mathbf{Q}^{-1}\mathbf{H}^T, \tag{4}$$

where $\mathbf{H} = [\mathbf{h}_1, ..., \mathbf{h}_{N_t}]$ is an $N_p \times N_t$ (N_p is the dimension of parameter set and N_t is the number of test points) matrix of vector parameter test points (note h_i is the vector parameter test point). For the zero-mean Gaussian data model mentioned in (1), it is required that $s_i = 1/2$ for all i [5]. In this case the (i, j)th element of the $N_t \times N_t$ matrix $\mathbf{Q}$ is given by

$$[\mathbf{Q}]_{ij} = 2 \cdot \frac{\exp\left\{\mu\left(1/2, \mathbf{h_i} - \mathbf{h_j}\right)\right\} - \exp\left\{\mu\left(1/2, \mathbf{h_i} + \mathbf{h_j}\right)\right\}}{\exp\left\{\mu\left(1/2, \mathbf{h_i}\right)\right\} \cdot \exp\left\{\mu\left(1/2, \mathbf{h_j}\right)\right\}}. \tag{5}$$

As derived in Ref. [10], computation of the WWB relies upon evaluating:

$$\mu\left(1/2, \mathbf{h}\right) = \ln\left[\int_{\Theta} \mathrm{d}\boldsymbol{\theta} \frac{p^{1/2}\left(\boldsymbol{\theta} + \mathbf{h}\right) p^{1/2}\left(\boldsymbol{\theta}\right)}{\prod_{m=1}^{M} \eta^L\left(f_m, \boldsymbol{\theta}, \mathbf{h}\right)}\right], \tag{6}$$

where $p(\boldsymbol{\theta})$ is the prior probability density and $\eta(f_m, \boldsymbol{\theta}, \mathbf{h})$ is given by

$$\eta(f_m, \boldsymbol{\theta}, \mathbf{h}) = |\mathbf{K_R}(f_m, \boldsymbol{\theta}+\mathbf{h})|^{1/2} |\mathbf{K_R}(f_m, \boldsymbol{\theta})|^{1/2} \cdot \left|(1/2)\,\mathbf{K_R^{-1}}(f_m, \boldsymbol{\theta}+\mathbf{h}) + (1/2)\,\mathbf{K_R^{-1}}(f_m, \boldsymbol{\theta})\right|, \quad (7)$$

where $|\cdot|$ denotes the matrix determinant.

Define

$$A(f_m, \boldsymbol{\theta}) = \frac{\sigma_b^2(f_m)\,\|\mathbf{G}(f_m, \theta)\|^2}{\sigma_b^2(f_m)\,\|\mathbf{G}(f_m, \theta)\|^2 + \sigma_n^2(f_m)}, \quad (8)$$

$$B(f_m, \boldsymbol{\theta}, \mathbf{h}) = \frac{\sigma_b^2(f_m)\,\|\mathbf{G}(f_m, \theta, \mathbf{h})\|^2}{\sigma_b^2(f_m)\,\|\mathbf{G}(f_m, \theta, \mathbf{h})\|^2 + \sigma_n^2(f_m)}, \quad (9)$$

and

$$C(f_m, \boldsymbol{\theta}, \mathbf{h}) = \mathbf{g}^{\dagger}(f_m, \boldsymbol{\theta})\,\mathbf{g}(f_m, \boldsymbol{\theta}+\mathbf{h}), \quad (10)$$

where $\|\cdot\|$ and $(\ )^{\dagger}$ represent the norm of the complex vector and Hermitian transposition, respectively, and $\mathbf{g}(f_m, \boldsymbol{\theta})$ is the normalized Green's function. Note that A and B are determined by the signal-to-noise ratios under $\boldsymbol{\theta}$ and $\boldsymbol{\theta}+\mathbf{h}$, respectively, and C defines a signal field correlation. We then have

$$\eta(f_m, \boldsymbol{\theta}, \mathbf{h}) = \frac{1}{\sqrt{(1-A)(1-B)}} \cdot \left(1 - \frac{A+B}{2} + \frac{AB}{4}\left(1-|C|^2\right)\right). \quad (11)$$

IV. The Matched-Covariance Estimator

The expression in (11) reminds one that η has a similar structure embedded in MVDR. Note that, given the problem formularization in Section II. and consider only the single-frequency case in the following simulation, the MVDR output power can be written as [1]:

$$\mathrm{S_{MVDR}}\left(\hat{\boldsymbol{\theta}}\right) = \left[\mathbf{g}^{\dagger}\left(\hat{\boldsymbol{\theta}}\right)\mathbf{K_R}(\boldsymbol{\theta}_T)\mathbf{g}\left(\hat{\boldsymbol{\theta}}\right)\right]^{-1}. \quad (12)$$

Rewrite (12) in terms of the signal-to-noise ratio and the signal field correlation as (7) :

$$\mathrm{S_{MVDR}}\left(\hat{\boldsymbol{\theta}}\right) = \sigma_n^2 \cdot \frac{1 + \frac{\sigma_b^2\|\mathbf{G}(\boldsymbol{\theta}_T)\|^2}{\sigma_n^2}}{1 + \frac{\sigma_b^2\|\mathbf{G}(\boldsymbol{\theta}_T)\|^2}{\sigma_n^2}\left(1-|C|^2\right)}, \quad (13)$$

where $C = \mathbf{g}^{\dagger}(\boldsymbol{\theta}_T)\,\mathbf{g}\left(\hat{\boldsymbol{\theta}}\right)$.

From (11) we can see that the term of $\frac{1}{\eta(\theta,h)}$ has a structure similar to (13). The $1-|C|^2$ term leads to side lobe cancellation, as discussed in [1]. This similar "estimator-subtractor" structure in MVDR and WWB stimulates us to develop a new estimator for MFP from (7) as:

$$\mathrm{S_{MCE}}\left(\hat{\boldsymbol{\theta}}\right) = \frac{1}{\left|\mathbf{K_R}\left(\hat{\boldsymbol{\theta}}\right)\right|^{1/2} \cdot |\mathbf{K_R}(\boldsymbol{\theta})|^{1/2}} \cdot \frac{1}{\left|\frac{1}{2}\mathbf{K_R^{-1}}\left(\hat{\boldsymbol{\theta}}\right) + \frac{1}{2}\mathbf{K_R^{-1}}(\boldsymbol{\theta})\right|}, \quad (14)$$

where $\mathbf{K_R}\left(\hat{\boldsymbol{\theta}}\right)$ and $\mathbf{K_R}(\boldsymbol{\theta})$ are scanning and sampled signal covariance matrix, respectively, parameterized by the parameter set $\boldsymbol{\theta}$. The estimate of $\boldsymbol{\theta}$ is determined by locating the peak of (14). Given a known covariance matrix and define

$$A(\boldsymbol{\theta}) = \frac{\sigma_b^2\|\mathbf{G}(\boldsymbol{\theta})\|^2}{\sigma_b^2\|\mathbf{G}(\boldsymbol{\theta})\|^2 + \sigma_n^2}, \quad (15)$$

$$B\left(\hat{\boldsymbol{\theta}}\right) = \frac{\sigma_b^2\left\|\mathbf{G}\left(\hat{\boldsymbol{\theta}}\right)\right\|^2}{\sigma_b^2\left\|\mathbf{G}\left(\hat{\boldsymbol{\theta}}\right)\right\|^2 + \sigma_n^2}, \quad (16)$$

$$C\left(\boldsymbol{\theta}, \hat{\boldsymbol{\theta}}\right) = \mathbf{g}^{\dagger}(\boldsymbol{\theta})\,\mathbf{g}\left(\hat{\boldsymbol{\theta}}\right), \quad (17)$$

the MCE output can be stated by

$$\mathrm{S_{MCE}}\left(\hat{\boldsymbol{\theta}}\right) = \frac{\sqrt{(1-A)(1-B)}}{1 - \frac{A+B}{2} + \frac{AB}{4}\left(1 - \left|C\left(\boldsymbol{\theta}, \hat{\boldsymbol{\theta}}\right)\right|^2\right)}, \quad (18)$$

We can see that Eqs. (15), (16) and (17) have a similar form as (8), (9) and (10) respectively. Among them Eqs. (15) and (16) are signal-to-noise ratio terms, and Eq. (17) is a signal ambiguity function term. Comparing (18) to (12), MCE and MVDR have the same "estimate-subtract" structure "$1-|C|^2$" which can realize adaptive sidelobe cancellation.

To facilitate further comparison in the next section, we notice that the maximum likelihood estimate output under the spatially-white noise background (as specified in Section II) is to maximize the logarithm of the conditional pdf:

$$p(\mathbf{R}|\boldsymbol{\theta}) = \frac{1}{|\pi\mathbf{K_R}(\boldsymbol{\theta})|^L} \cdot \prod_{l=1}^{L} \exp\left(-\mathbf{R}_l^{\dagger}\mathbf{K_R^{-1}}(\boldsymbol{\theta})\,\mathbf{R}_l\right). \quad (19)$$

V. Simulations

Performance analysis of MCE is implemented, in comparison to MLE and MVDR, for source localization in a shallow water environment chosen from the 2001 Asian Seas International Acoustic Experiment (ASIAEX) which is shown in Fig. 1. Firstly we draw the ambiguity outputs of MCE, MLE and MVDR. The covariance matrix is assumed unknown and adaptively estimated from a number of data snapshots. The results, under SNR = 5 dB, are shown in Fig. 2 and Fig. 3 with the snapshot number $L = 20$ and $L = 40$, respectively.

The ambiguity output of MCE is similar to MVDR having a more focus mainlobe and much lower sidelobe than MLE, due to the side lobe suppression resulted from ability of the "estimator-subtract" structure. Comparing Fig. 2 to Fig.3, the baseline of MVDR grows higher when the snapshot number is cutted into half, however the baseline of MCE stays almost the same.

The MSE of source range estimation is evaluated as a function of SNR, presented in Fig. 4 and Fig. 5, and the evaluation is included with the predication of Bayesian Cramer-Rao Bound (BCRB) and WWB, as well as the MVDR and MLE simulation results from 3000 Monte Carlo trails. To fit into the Bayesian framework of the BCRB and WWB, the

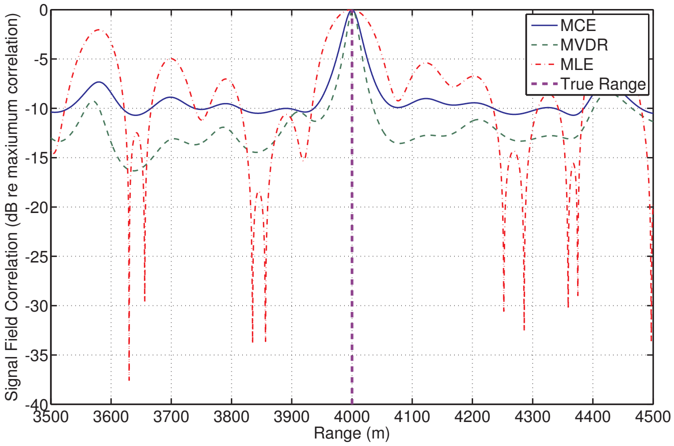

Fig. 2. Ambiguity Output of MCE, MLE and MVDR ($L = 20$).

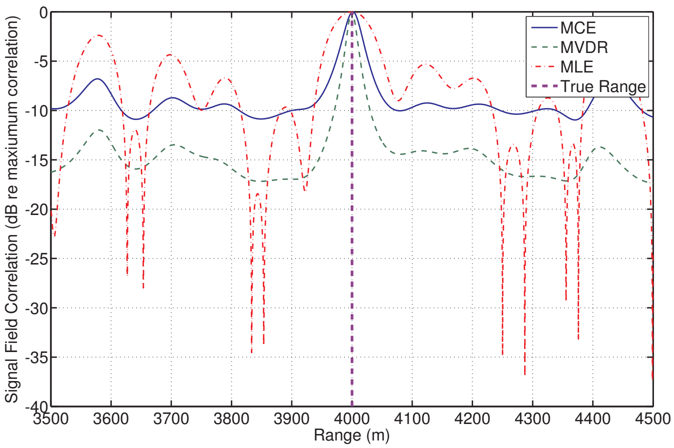

Fig. 3. Ambiguity Output of MCE, MLE and MVDR ($L = 40$).

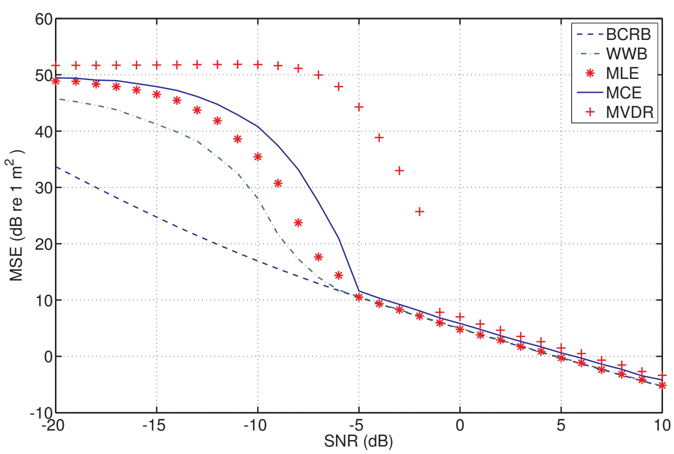

Fig. 4. Perform evaluation for source range estimation ($L = 40$).

true source range for synthesizing the observation is uniformly chosen across the given interval of [3500,4500]m.

Fig. 4, with the snapshot number $L = 40$, shows that MCE performs equally well with MLE in the sense of MSE, especially in high SNR. Compared with MVDR, MCE outperforms at least 4 dB at high SNR and almost 33 dB at moderate SNR. For the threshold SNR concern, MCE achieves the same threshold SNR with MLE, which is 4 dB lower than MVDR.

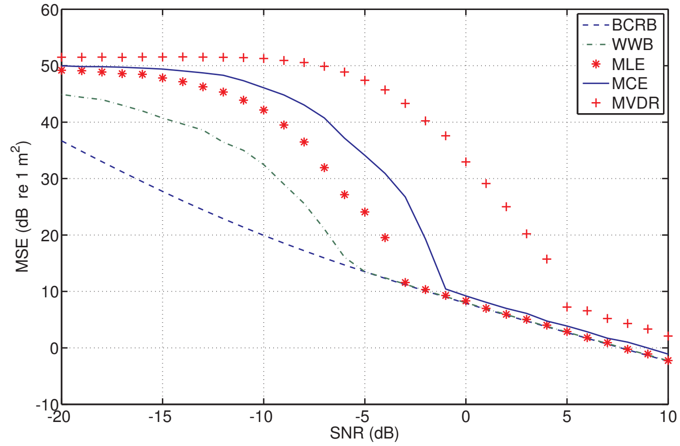

Fig. 5. Perform evaluation for source range estimation ($L = 20$).

From Fig. 5 we could see that with snapshot number cut into half, MCE still performes close to MLE, which means the error in covariance estimation only leads a moderate performance loss for MCE. However, the MSE of MVDR is at least 4 dB higher than MCE in high SNR and almost 28 dB higher in moderate SNR. This time, the threshold SNR of MCE was 2 dB higher than MLE which may be caused by the noise spreading into the signal subspace (rank increase), but it's still 6 dB lower than MVDR. This phenomenon reveals that MCE is quite robust against the snapshot deficiency and can tolerate some error in covariance estimation.

VI. Conclusion

In this paper, we bring in the new parameter estimator from the derivation of the Weiss-Weinstein bound. The estimator matches the modeled covariance matrix with the true one, and because the covariance matrix completely characterizes the probability density function in the problem, it can be understood as statistical matching. The ASIAEX shallow water waveguide simulation results show that: 1) MCE owns a high spatial distinguishability, like MVDR, with a focused peak in ambiguity output; 2) MCE can almost achieve the same MSE as MLE over all SNR and outperform MVDR especially in moderate to high SNR levels; 3) the threshold SNR of MCE is lower than that of MVDR and stays close to MLE, which means MCE has a stronger noise suppression ability; 4) like MLE, the performance of MCE is not seriously degraded even though the covariance matrix is estimated from limited datasets. Overall, MCE achieves a trade-off between spatial resolution and performance robustness against snapshot deficiency.

MCE is essentially a model-based method, requiring matching of both signal and noise statistics. To fully understand its performance, some further testing is certainly needed under other signal and noise conditions. For example, the current development only considers the spatially-white noise processes;

generalization to spatially-correlated noises and investigation of its sensitivity to noise covariance mismatch is certainly desired.

ACKNOWLEDGMENT

This work was supported by Chinese High-Tech Program under Grant 2012AA090901 and National Scientific Supporting Program under Grant 2012BAH34B03.

REFERENCES

[1] A. B. Baggeroer, W. A. Kuperman, and H. Schmidt, "Matched field processing: Source localization in correlated noise as an optimum parameter estimation problem," *J. Acoust. Soc. Am.*, vol. 83, no. 2, pp. 571–587, 1988.

[2] A. B. Baggeroer and H. Schmidt, "Parameter estimation theory bounds and the accuracy of full field inversions," in *Full Field Inversion Methods in Ocean and Seismo-Acoustics*, O. Diachok, Ed. Springer, 1995, pp. 79–84.

[3] A. Baggeroer, W. Kuperman, and P. Mikhalevsky, "An overview of matched field methods in ocean acoustics," *IEEE J. Oceanic Eng.*, vol. 18, no. 4, pp. 401–424, 1993.

[4] S. M. Kay, *Fundamentals of Statistical Signal Processing: Estimation Theory*, E. Cliffs, Ed. NJ: Prentice-Hall, 1993.

[5] W. Xu, "Performance bounds on matched-field methods for source localization and estimation of ocean environment parameters," Ph.D. dissertation, Mass. Inst. Technol., MA, 2001.

[6] K. Yang, Y. Ma, C. Sun, J. H. Miller, and G. R. Potty, "Multistep matched-field inversion for broad-band data from asiaex2001," *IEEE J. Oceanic Eng.*, vol. 29, no. 4, pp. 964–972, Oct. 2004.

[7] W. Xu, A. B. Baggeroer, and H. Schmidt, "Performance analysis for matched-field source localization: Simulations and experimental results," *IEEE J. Oceanic Eng.*, vol. 31, no. 2, pp. 325–344, 2006.

[8] A. B. Baggeroer and H. Schmidt, "Cramer-rao bounds for matched field tomography and ocean acoustic tomography," in *Proc. ICASSP*, 1995, pp. 2763–2766.

[9] E. Weinstein and A. J. Weiss, "A general class of lower bounds in parameter estimation," *IEEE Transactions on Information Theory*, vol. 34, no. 2, pp. 338–342, 1988.

[10] W. Xu, A. B. Baggeroer, and C. D. Richmond, "Bayesian bounds for matched-field parameter estimation," *IEEE Trans. Signal Process.*, vol. 52, no. 12, pp. 3293–3305, Dec 2004.